

Application of PDF methods to compressible turbulent flows

B. J. Delarue^{a)} and S. B. Pope

Sibley School of Mechanical and Aerospace Engineering, Cornell University, Ithaca, New York 14853

(Received 30 September 1996; accepted 13 May 1997)

A particle method applying the probability density function (PDF) approach to turbulent compressible flows is presented. The method is applied to several turbulent flows, including the compressible mixing layer, and good agreement is obtained with experimental data. The PDF equation is solved using a Lagrangian/Monte Carlo method. To accurately account for the effects of compressibility on the flow, the velocity PDF formulation is extended to include thermodynamic variables such as the pressure and the internal energy. The mean pressure, the determination of which has been the object of active research over the last few years, is obtained directly from the particle properties. It is therefore not necessary to link the PDF solver with a finite-volume type solver. The stochastic differential equations (SDE) which model the evolution of particle properties are based on existing second-order closures for compressible turbulence, limited in application to low turbulent Mach number flows. Tests are conducted in decaying isotropic turbulence to compare the performances of the PDF method with the Reynolds-stress closures from which it is derived, and in homogeneous shear flows, at which stage comparison with direct numerical simulation (DNS) data is conducted. The model is then applied to the plane compressible mixing layer, reproducing the well-known decrease in the spreading rate with increasing compressibility. It must be emphasized that the goal of this paper is not as much to assess the performance of models of compressibility effects, as it is to present an innovative and consistent PDF formulation designed for turbulent inhomogeneous compressible flows, with the aim of extending it further to deal with supersonic reacting flows. © 1997 American Institute of Physics. [S1070-6631(97)01709-1]

I. INTRODUCTION

Over the past few years, renewed interest in supersonic aircraft and high-speed combustion has emphasized the need for research in the field of compressible turbulence. Important theoretical results have been established and reviewed,¹ allowing a better understanding of the complex phenomena involved in compressible turbulence. Extensive experimental work has been conducted, especially in the case of the plane compressible mixing layer.²⁻⁹ In the turbulence modelling community, the limitations of existing incompressible turbulence models have been established.¹⁰ Second-order closures have been designed to represent explicit compressibility effects, such as the compressible dissipation and the pressure-dilatation correlation.¹¹⁻¹⁸ The need for future research, in both understanding and modelling the effects of compressibility on turbulence, has been clearly established.^{10,19}

For flows involving combustion, probability density function (PDF) methods have demonstrated their ability to treat the important processes of reaction and convection exactly,²⁰ making transport and reaction models used in ordinary PDE solvers unnecessary. The modelled transport equation for the joint PDF of velocity and composition has been successfully solved, using sets of stochastic particles with time-evolving properties to model fluid particles.^{21,22} Recent works include the development of models for the velocity-dissipation joint PDF.^{23,24} However, the majority of applications is limited to low Mach number flows and, without coupling to a finite-volume type solver to obtain quanti-

ties such as the mean pressure, to flows with weak pressure gradients.

Only recently have PDF methods been applied to flows with pressure-induced density variations,²⁵⁻²⁷ requiring in general (except reference 27) coupling with a finite-volume solver of some kind. The problem of determining the mean pressure directly from the particle properties (i.e., without a finite-volume solver) is closely related to the difficulties encountered in trying to extend PDF formulation to complex compressible flows.

The objective of the present work is to extend the existing PDF models to compressible reacting flows with arbitrary pressure gradients, with the aim of developing a stand-alone method to solve for the joint PDF of all relevant flow variables, including the dissipation rate of turbulent kinetic energy, without coupling with a pressure algorithm. By doing so we hope to exploit fully, in a simple and computationally efficient way, the remarkable potential offered by PDF methods to solve for complex turbulent reacting flows.

For the definition of the method, henceforth, we restrict ourselves to nonreacting flows. It is believed, however, that extension of the method to account for the reaction will be straightforward. The method has been successfully implemented for homogeneous compressible flows (hence it deals with unsteady flows without coupling with a finite-volume solver, a feature displayed only by recent work using smoothed particle hydrodynamics²⁷), and statistically stationary inhomogeneous flows. A unique feature of the method is the inclusion in the joint PDF of two extra thermodynamic variables, namely the pressure and the internal energy. Hence, all statistics of the flow, including the mean pressure, can be determined directly from the particle properties. A

^{a)}Present address: Electricité de France, Laboratoire National d'Hydraulique, 78401 Chatou, France.

finite-volume type solver is therefore unnecessary. In addition, models have been derived from existing Reynolds stress closures to account for the compressible dissipation and the pressure–dilatation correlation.

In section II we review some general effects of compressibility on turbulent flows, as well as second-order closures from which our PDF formulation is inspired. It is emphasized that the purpose of this work is neither to develop new models for compressibility effects on turbulence, nor to test existing models, but to develop an innovative and consistent PDF formulation designed for high-speed combustion. In section III we detail the PDF formulation which is the object of this work, summarizing briefly the general idea behind PDF methods, then defining our stochastic variables and the corresponding stochastic differential equations (SDE). In section IV we present results for homogeneous flows. In section V, we extend the model to inhomogeneous flows. At this point a comparison is made between model results and experimental data in the supersonic mixing layer case.

II. MODELS FOR THE EFFECTS OF COMPRESSIBILITY ON TURBULENCE

In compressible reacting flows, density variations arise because of variations in chemical composition, and of temperature and pressure fluctuations. While all these effects contribute to create nonzero dilatation rates, only the latter are termed compressibility effects. In the following discussion, we consider an inert flow and therefore ignore the effects of a chemical reaction on the density.

Consider the equation for turbulent kinetic energy in compressible flow:

$$\langle \rho \rangle \frac{\partial k}{\partial t} + \langle \rho \rangle \bar{U}_i \frac{\partial k}{\partial x_i} = T + P + \Pi_d - \langle \rho \rangle \varepsilon - \langle u_i'' \rangle \left(\frac{\partial \langle p \rangle}{\partial x_i} - \frac{\partial \langle \tau_{ij} \rangle}{\partial x_j} \right), \quad (1)$$

where

$$T = - \frac{\partial}{\partial x_i} \left(\frac{1}{2} \langle \rho \rangle \overline{u_j'' u_j'' u_i''} + \langle p' u_i'' \rangle - \langle u_j'' \tau_{ij}' \rangle \right)$$

is the transport term,

$$P = - \langle \rho \rangle \overline{u_i'' u_j''} \frac{\partial \bar{U}_i}{\partial x_j}$$

is the production term,

$$\Pi_d = \left\langle p' \frac{\partial u_i'}{\partial x_i} \right\rangle$$

is the trace of the pressure-rate of strain correlation, also called *pressure dilatation*, and ε is the viscous dissipation. In (1), the brackets correspond to Reynolds averages and the primes to fluctuations about these averages, while the tildes and double primes stand for Favre averages and fluctuations, respectively. It has been shown^{11,14} that the viscous dissipation can be split into two terms:

$$\varepsilon = \varepsilon_s + \varepsilon_d,$$

where $\varepsilon_s = \nu \langle \omega_i' \omega_i' \rangle$ is the standard solenoidal dissipation, and $\varepsilon_d = 4/3 \nu \langle u_i'^2 \rangle$ is the so-called *dilatation dissipation*, which is clearly zero in incompressible flows, and strictly positive in compressible flows, thus amounting to extra dissipation. We see that in (1) three explicit terms arising from compressibility need to be modelled: ε_d , Π_d , and the last term, which arises because the Reynolds averages $\langle u_i'' \rangle$ of Favre fluctuations are nonzero. The last term is probably very small in flows without large pressure gradients and away from walls. We therefore choose to neglect it. We need, however, to model the other two.

For the dilatation dissipation, we use the model of Sarkar *et al.*¹¹ relating ε_d to ε_s in the following way:

$$\varepsilon_d = C_d M_t^2 \varepsilon_s, \quad (2)$$

where $M_t^2 = 2k/\bar{a}^2$ is the turbulent Mach number squared, \bar{a} being the mean speed of sound. This model was developed for $M_t \ll 1$. The constant C_d is of order 1. Equation (2) relates the dilatation dissipation to the solenoidal dissipation. It has been argued^{11,14} that the energy cascade responsible for the latter is moderately affected by compressibility, therefore standard incompressible models for the solenoidal dissipation can be used in the present situation.

For the pressure dilatation, we use Zeman's model,¹⁵ which can be summarized in the following two equations:

$$\Pi_d = - \frac{1}{2 \gamma \langle \rho \rangle} \frac{D \langle p'^2 \rangle}{Dt}, \quad (3)$$

$$\frac{D \langle p'^2 \rangle}{Dt} = - \frac{\langle p'^2 \rangle - p_e^2}{\tau_a}. \quad (4)$$

The first equation is valid in homogeneous turbulence for $M_t \ll 1$, and for high Reynolds and Péclet numbers. The second equation is fully modelled, relying on the results of Sarkar *et al.*,^{11,28} and stating that pressure variance relaxes to an equilibrium level p_e on the acoustic time scale τ_a . These two model quantities are defined in Zeman.¹⁵ The pressure–dilatation is expected to be important in nonequilibrium flows, namely in flows with a strong dependence on initial conditions, for instance decaying isotropic turbulence. It is expected to be of lesser importance in equilibrium flows, for instance most free shear flows without shocks. To date, most models for Π_d ^{12,15,16} are restricted to weakly inhomogeneous turbulence.

The models for both ε_d and Π_d are restricted to flows with $M_t \ll 1$. In our calculations, for example, in mixing layers with free stream Mach numbers as high as 6.5, we never encountered values of M_t above 0.5, which has been considered to fall within the range of applicability of these models.

The above discussion is centered exclusively on modelling from the point of view of the turbulent kinetic energy equation, and not from the Reynolds stresses equation. The models we have chosen will affect the turbulence in an isotropic manner. Though it is known at this point^{19,10} that compressibility also, and probably chiefly, affects the turbulence by modifying the deviatoric pressure-rate of strain correlation so that the redistribution of energy does not function as well when the compressibility level is high, resulting in increased anisotropies in the normal stresses and decreased an-

isotropy in the shear stresses,¹⁹ we have chosen not to modify our incompressible models for the pressure-rate of strain correlation. As of yet, no general model is available for this term, and it is still the object of ongoing research. Furthermore, the above models — in particular the dilatation dissipation model — have been shown to reproduce well-known compressibility effects on turbulence such as the decrease in the spreading rate of a mixing layer when compressibility increases.²⁹ It must be said, however, that recent results show that the decrease in the growth rate comes mainly from the pressure-rate of strain correlation.³⁰ It is therefore necessary to keep in mind that the models we are using may not be valid for a wide variety of flows, and may not be representing the dominant physical effects of compressibility on turbulence. Let us emphasize at this point, however, that the emphasis of this work is not on modelling, but on extending the domain of applicability of PDF methods to compressible flows. As better models are developed for the effects of compressibility on turbulence, it will be straightforward to incorporate them in our PDF formulation.

To complete this section, we need to discuss the equations for the two thermodynamic variables necessary to describe the state of the fluid. The continuity equation plays a different role in PDF/Monte Carlo methods than in second-order closure methods. Its satisfaction is a requirement if the particle ensemble — introduced in the next section — is to be a consistent representation of the fluid,²⁰ and not a means for obtaining the fluid density if the velocity field is known. Therefore we do need two thermodynamic variables, both different from the density, to describe the flow. For reasons that will be given in the next section, we choose the pressure, p , and the specific internal energy, e .

The evolution equations for the means, $\langle p \rangle$ and \tilde{e} , can be derived from the first law of thermodynamics and the equation of state for an ideal gas. They are

$$\frac{\partial \langle p \rangle}{\partial t} + \langle U_i \rangle \frac{\partial \langle p \rangle}{\partial x_i} = \langle \rho \rangle (\gamma - 1) \varepsilon - \gamma \langle p \rangle \langle \Delta \rangle - (\gamma - 1) \Pi_d - \frac{\partial \langle p' u_i' \rangle}{\partial x_i}, \quad (5)$$

$$\langle \rho \rangle \frac{\partial \tilde{e}}{\partial t} + \langle \rho \rangle \tilde{U}_i \frac{\partial \tilde{e}}{\partial x_i} = \langle \rho \rangle \varepsilon - \langle p \rangle \langle \Delta \rangle - \Pi_d - \frac{\partial \langle \rho \rangle u_i'' e''}{\partial x_i}. \quad (6)$$

The fluid is an ideal gas, γ being the ratio of specific heats, and $\Delta = U_{i,i}$ is the dilatation rate. In the above equations, we neglected terms corresponding to molecular heat flux and mean viscous stress, both of which will be negligible in the flows of interest in this paper. The turbulent pressure fluxes in (5) and energy fluxes in (6) are unclosed. In addition, we need to determine the Reynolds average of the dilatation rate Δ . In second-order closure methods, the mean velocity equations only involve Favre averages of the velocity, and it is necessary to model the turbulent mass fluxes $\langle \rho' u_i' \rangle$ to switch between Favre and Reynolds averaging. Using the PDF formulation detailed in the next section, *no modelling effort is required* in this respect. The turbulent mass, energy,

and pressure fluxes are all in closed form and hence the equations for the thermodynamic variables require no additional models.

III. THE PDF FORMULATION

A. The Eulerian mass–density function

In a turbulent compressible flow, we may look at the flow properties U , ω (turbulent frequency), e , and p at any fixed location x and time t as random variables. If we denote the sample space variables associated with these random flow variables with a hat ($\hat{\cdot}$), we define the one-point Eulerian mass–density function \mathcal{F} as

$$\mathcal{F}(\hat{U}, \hat{\omega}, \hat{e}, \hat{p}; x, t) = \rho(\hat{e}, \hat{p}) \langle \delta(U(x, t) - \hat{U}) \delta(\omega(x, t) - \hat{\omega}) \delta(e(x, t) - \hat{e}) \delta(p(x, t) - \hat{p}) \rangle. \quad (7)$$

In this definition δ is the Dirac delta function.

Statistics of the flow are computed with the moments of \mathcal{F} . Three important properties of \mathcal{F} are

$$\int \mathcal{F} d\hat{U} d\hat{\omega} d\hat{e} d\hat{p} = \langle \rho(x, t) \rangle, \quad (8)$$

$$\int \mathcal{F} Q^*(\hat{U}, \hat{\omega}, \hat{p}, \hat{e}) d\hat{U} d\hat{\omega} d\hat{p} d\hat{e} = \langle \rho(x, t) Q(x, t) \rangle = \langle \rho \rangle \tilde{Q}, \quad (9)$$

$$\int \mathcal{F} \langle Q | \hat{U}, \hat{\omega}, \hat{p}, \hat{e} \rangle d\hat{U} d\hat{\omega} d\hat{p} d\hat{e} = \langle \rho \rangle \tilde{Q}. \quad (10)$$

In the above system Q^* is any function of the flow variables U , ω , e , p , and $Q = Q(x, t)$ is defined as

$$Q(x, t) = Q^*(U(x, t), \omega(x, t), e(x, t), p(x, t)).$$

If in eq. (9) we replace Q^* by Q^*/ρ , we see that the integration over the sample space yields the Reynolds average, instead of the Favre average:

$$\int \mathcal{F} \frac{1}{\rho(\hat{e}, \hat{p})} Q^*(\hat{U}, \hat{\omega}, \hat{p}, \hat{e}) d\hat{U} d\hat{\omega} d\hat{p} d\hat{e} = \left\langle \frac{1}{\rho} \rho Q \right\rangle = \langle Q \rangle.$$

Therefore, knowing \mathcal{F} we can switch freely between Favre and Reynolds averages. Hence, as alluded to in the previous section, no modelling of the mass fluxes is necessary.

B. Particle representation

In a Monte Carlo simulation of a flow with constant total mass M , \mathcal{F} is represented by an ensemble of N stochastic particles, each of mass $\Delta m = M/N$, which model fluid particles. The assumption of constant total mass does not affect the generality of the following analysis. In an actual numerical implementation, both the particle number N and the particle mass Δm are allowed to vary, but taking this into account at this point would make the analysis unnecessarily complicated.

In our representation, each stochastic particle i has a position $x^{(i)}$, a velocity $U^{(i)}$, a turbulent frequency $\omega^{(i)}$, a pressure $p^{(i)}$, and a specific internal energy $e^{(i)}$. All these

properties depend only on time t , and evolve according to modelled evolution equations. The discrete Lagrangian mass–density function is defined as

$$\begin{aligned} \mathcal{F}_N(\hat{U}, \hat{\omega}, \hat{e}, \hat{p}, x; t) = \Delta m \sum_{i=1}^N \delta(U^{(i)} - \hat{U}) \delta(\omega^{(i)} - \hat{\omega}) \\ \times \delta(e^{(i)} - \hat{e}) \delta(p^{(i)} - \hat{p}) \delta(x^{(i)} - x). \end{aligned} \quad (11)$$

The moments of \mathcal{F}_N give the statistics of particle properties. We require these to model statistics of the flow.

Each stochastic particle is supposed, at the location which it is occupying, to represent a single realization of the flow. Therefore all particles are statistically equivalent, and we can define the particle mass–density q as

$$q = \Delta m \sum_{i=1}^N \langle \delta(x^{(i)} - x) \rangle = M \langle \delta(x^* - x) \rangle, \quad (12)$$

where x^* is the position of any stochastic particle in $1, \dots, N$. This quantity is analogous to the fluid density ρ .

For the particle system to be a valid representation of the flow, we require the correspondence

$$\tilde{f} = \langle \mathcal{F}_N \rangle / q, \quad (13)$$

where $\tilde{f} = \mathcal{F} / \langle \rho \rangle$ is the Eulerian density-weighted joint PDF of fluid properties. This expression implies that the mean of a particle property conditional upon the particle location, obtained by computing the moments of $\langle \mathcal{F}_N \rangle / q$, is equal to the Favre average of the corresponding fluid property at that location. Or, if $\alpha(x, t)$ is a fluid property, and $\alpha^*(t)$ the corresponding stochastic particle property, then we have

$$\langle \alpha^* | x \rangle = \alpha(\tilde{x}, t), \quad (14)$$

where the left-hand side is an abbreviation for the conditional expectation $\langle \alpha^*(t) | x^*(t) = x \rangle$.

C. Evolution equations for the particle properties

In this section we give the evolution equations for all particle properties x^* , e^* , p^* , U^* , and ω^* . These are written as stochastic differential equations (SDE) in which $d\alpha^* = d\alpha^*(t)$ denotes the infinitesimal increment $\alpha^*(t+dt) - \alpha^*(t)$ for any stochastic particle property α^* .

The particles model fluid particles, and hence move with their own velocity:

$$dx^* = U^* dt. \quad (15)$$

The internal energy evolves according to the first law of thermodynamics:

$$de^* = \varepsilon dt - p^* dv^*. \quad (16)$$

In the above equation, v^* refers to the specific volume of the stochastic particle, related to e^* and p^* through the equation of state, which for an ideal gas with constant specific heats reads as

$$p^* v^* = (\gamma - 1) e^*. \quad (17)$$

Therefore dv^* is known if dp^* and de^* are known. Equation (16), as was stated above, is derived from the first law of thermodynamics: the first term on the right-hand side is the heat added through dissipative work, and the second term is the pressure work.

The dissipation ε is equal to $k\Omega(1 + C_d M_t^2)$, where Ω is a quantity derived from the turbulent frequency ω^* . More detail on Ω is to be found in Jayesh and Pope,³¹ and the evolution equation for ω^* is given at the end of this section. No model is incorporated in eq. (16) to account for molecular transport. We are restricting our analysis to flows with high Reynolds and Péclet numbers.

The pressure equation is fully modelled. We write it in a general form:

$$dp^* = p^*(A dt + B dW). \quad (18)$$

We see that this SDE involves a Wiener process $W(t)$, which has the following properties:

$$\langle dW \rangle = 0,$$

$$\langle dW^2 \rangle = dt.$$

For a more exhaustive review of the properties of the Wiener process, see Pope.²⁰ The two model coefficients A and B are given by

$$A = \frac{\varepsilon}{e^*} + \frac{B^2}{2} \left(1 + \frac{1}{\gamma} \right) - \gamma \frac{\partial \langle U_i \rangle}{\partial x_i} + (\gamma - 1) \Omega_A (p^* - \langle p \rangle), \quad (19)$$

$$B^2 = \frac{p_e^2}{\tau_a} \frac{1}{\theta} \frac{1}{(\langle \rho \rangle \tilde{a})^2} \frac{1}{e^*}. \quad (20)$$

In the above equations, Ω_A , p_e , and τ_a are given by Zeman¹⁵ and $\theta = 1 - \gamma^{-1}$.

The coefficients A and B in (19) and (20) are determined so that the following two conditions are satisfied: (i) the specific volume v^* satisfies, in the mean, the mean continuity equation, and (ii) the pressure dilatation correlation has the same form as in Zeman's model,¹⁵ obtained by combining eqs. (3) and (4):

$$\Pi_d = \frac{\langle p'^2 \rangle - p_e^2}{2\tau_a \langle \rho \rangle \tilde{a}^2}. \quad (21)$$

This amounts to having the pressure variance evolve according to eq. (4), to first order in M_t^2 and in homogeneous flows. However, in arbitrary flows, as we will see, the PDF pressure variance equation is quite different, but the expression for Π_d is still eq. (21).

The form of Zeman's model for the pressure–dilatation is quite complicated. If a simpler, algebraic model such as Sarkar's¹² were to be used, the expressions for A and B would also become simpler. In the most general case, if f_d is the function of known flow statistics which gives the pressure–dilatation, then we can rewrite A as

$$A = \frac{\varepsilon}{e^*} - \gamma \frac{\partial \langle U_i \rangle}{\partial x_i} - \gamma \frac{f_d}{\langle \rho \rangle \langle p'^2 \rangle} (p^* - \langle p \rangle),$$

and B can be taken to be zero. These modifications are valid for any function f_d , including eq. (21). In the special case where the expression for this function contains terms which are always negative — such as the term in p_e in Zeman's model — these terms will be preferably incorporated in B , resulting in a nonzero value for this model coefficient. This is the approach taken in this paper. If, however, none of the terms in f_d is consistently negative, as is the case in Sarkar's model, B has to be zero, and A has to be given by the above expression.

A unique feature of this formulation is that averaging of the pressure work $p^* dv^*$ over the stochastic particles yields the pressure dilatation correlation *in closed form*. The PDF formulation preserves the physical meaning of Π_d as the mean of the fluctuating pressure work $p' dv'$. Hence, once the evolution equations for p^* and e^* are specified, no additional modelling is required to obtain the pressure dilatation.

There is a variety of ways to select the two thermodynamic variables needed to describe the state of the fluid.^{32,33} The choice of e and p is advantageous for the following reasons. There is a straightforward correspondence between the specific internal energy and the temperature in reacting flows, and the evolution equation for e^* can be derived from simple physical principles. The choice of p allows us to control the pressure variance $\langle p'^2 \rangle$ so that it evolves according to (4) in homogeneous turbulence and for low M_t , and therefore to represent the energy associated with pressure fluctuations in compressible flow in the same way as Zeman's model represents it.

The velocity evolves according to the simplified Langevin model,³⁴ modified to account for the presence of Π_d in the turbulent kinetic energy equation:

$$dU_i^* = -\frac{1}{\langle \rho \rangle} \frac{\partial \langle p \rangle}{\partial x_i} dt + \frac{1}{2k} \left(\frac{\Pi_d}{\langle \rho \rangle} - \varepsilon \left(1 + \frac{3}{2} C_0 \right) \right) (U_i^* - \bar{U}_i) dt + (C_0 \varepsilon)^{1/2} dW_i. \quad (22)$$

Accounts of the performance of this model can be found in Pope.³⁵ The value of the model constant C_0 is 2.1.

Finally, the turbulent frequency evolves according to the model equation of Jayesh and Pope:³¹

$$d\omega^* = -(\omega^* - \bar{\omega}) C_3 \Omega dt - \bar{\omega} \omega^* S_\omega dt + (2\sigma^2 \bar{\omega} \omega^* C_3 \Omega)^{1/2} dW. \quad (23)$$

Details on the model and a brief review of its performance can be found in Jayesh and Pope.³¹

The stochastic differential equations detailed above [(15), (16), (18), (22), and (23)] yield an evolution equation for \mathcal{F}_N/q with no unclosed terms, which constitutes a model for the evolution equation of the one-point density-weighted joint PDF \tilde{f} . The equations for the moments of \mathcal{F}_N/q constitute model equations for the corresponding moments of \tilde{f} . For instance, the evolution equation for $\langle e^* | x \rangle$ is strictly identical to (6), and the evolution equation for $\langle p \rangle = \langle p^* v^* | x \rangle / \langle v^* | x \rangle$ is identical to (5), with Π_d modelled

according to Zeman's model in both cases, and the turbulent pressure and energy fluxes in closed form. The modelled turbulent kinetic energy equation reads as

$$\langle \rho \rangle \frac{\partial k}{\partial t} + \langle \rho \rangle \bar{U}_i \frac{\partial k}{\partial x_i} = -\frac{\partial}{\partial x_i} \left(\frac{1}{2} \langle \rho \rangle u_j'' u_j'' u_i'' \right) - \langle \rho \rangle u_i'' u_j'' \frac{\partial \bar{U}_j}{\partial x_i} + \Pi_d - \langle \rho \rangle \varepsilon. \quad (24)$$

As we can see, the only terms that are not accounted for in this equation, let alone the terms we decided to neglect in the first section, are the pressure and viscous transport terms. Finally, the modelled pressure variance equation reads as

$$\frac{\partial \left(\frac{1}{2} \langle p'^2 \rangle \right)}{\partial t} + \langle U_i \rangle \frac{\partial \left(\frac{1}{2} \langle p'^2 \rangle \right)}{\partial x_i} = -\gamma \langle p'^2 \rangle \langle \Delta \rangle - \langle p' u_i' \rangle \frac{\partial \langle p \rangle}{\partial x_i} - \frac{1}{2} \frac{\partial}{\partial x_i} \langle p'^2 u_i' \rangle - \gamma \langle p \rangle \Pi_d + \langle \rho \rangle (\gamma - 1) \varepsilon p^{\overline{\gamma}}, \quad (25)$$

which we can compare with the true pressure variance evolution equation:¹

$$\frac{\partial \left(\frac{1}{2} \langle p'^2 \rangle \right)}{\partial t} + \langle U_i \rangle \frac{\partial \left(\frac{1}{2} \langle p'^2 \rangle \right)}{\partial x_i} = -\gamma \langle p'^2 \rangle \langle \Delta \rangle - \langle p' u_i' \rangle \frac{\partial \langle p \rangle}{\partial x_i} - \frac{1}{2} \frac{\partial}{\partial x_i} \langle p'^2 u_i' \rangle - \gamma \langle p \rangle \Pi_d - \frac{2\gamma - 1}{2} \langle p'^2 \Delta' \rangle. \quad (26)$$

As alluded to earlier, our model equation (25) is more complete than eq. (4) in inhomogeneous flows. It is very close to eq. (26) (in which we omitted terms coming from molecular transport). The only difference lies in the last term of each equation, which we will prove to be negligible in (25), and which scales like $M_t^2 \langle p \rangle \Pi_d$ in (26), and is therefore negligible compared to the $\langle p \rangle \Pi_d$ term. For the sake of clarity, we omitted in (25) terms of order M_t^2 or higher which we already know to be negligible.

IV. IMPLEMENTATION IN HOMOGENEOUS TURBULENCE

A. Decaying isotropic turbulence

The purpose of this section is to compare the performances of our formulation to those of a classical Reynolds stress closure using Zeman's and Sarkar's models. The only difference between PDF and second-order closure, in homogeneous isotropic turbulence, is that the pressure–dilatation Π_d is related to $\langle p'^2 \rangle$ by eq. (3) in the latter case, whereas it is obtained through direct averaging of $p^* dv^*$ in the former case. Since, as was said before, the model has been designed so as to have the same expression for Π_d [eq. (21)] in both cases, we need to check that $\langle p'^2 \rangle$ also has the same value, or that the last term in eq. (25) is small compared to Π_d — in

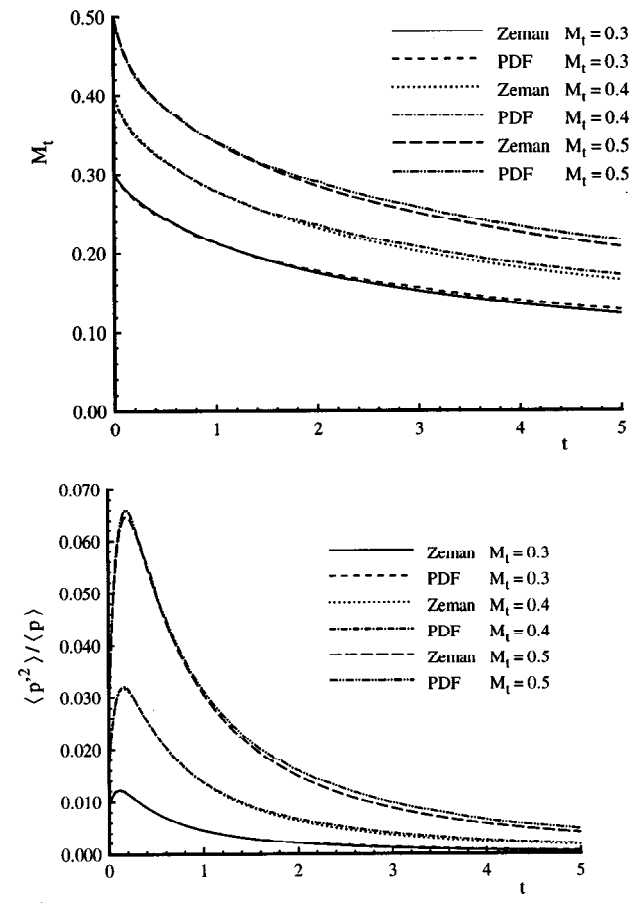


FIG. 1. Turbulent Mach number and normalized pressure variance versus time for the initial level of pressure fluctuations $\Pi_0=0.05$ and various values of the initial turbulent Mach number M_{t0} .

which case the evolution equations (4) and (25) will be virtually identical. Our results (Figs. 1 and 2) show that the agreement between the values of the pressure variance and other statistics of the flow (here M_t) in both methods is excellent. Our method therefore provides an excellent PDF equivalent of a Reynolds-stress closure incorporating Zeman's and Sarkar's models.

Figure 3 shows that the Favre and Reynolds averages can both be obtained with our method. Even in this case there is a significant difference between both quantities (displayed here for the specific internal energy, which is proportional to the temperature).

Decaying turbulence exhibits a strong dependence on initial conditions. For our problem, initial conditions depend upon two parameters only, because the initial level of density fluctuations is set to zero: the initial turbulent Mach number M_{t0} , and the initial level of pressure fluctuations Π_0 . Figure 1 corresponds to low Π_0 and high M_{t0} , figure 2 to the opposite situation. In both situations we observe a rapid exchange between pressure fluctuations and kinetic energy on the acoustic time scale τ_d , due to Π_d , followed by viscous decay of the turbulence.

B. Homogeneous shear flow

In this section, the mean shear $S = \tilde{U}_{1,2}$ has a constant value set to $(Sk/\varepsilon_s)_0 = 7.2$. We compare our results to DNS

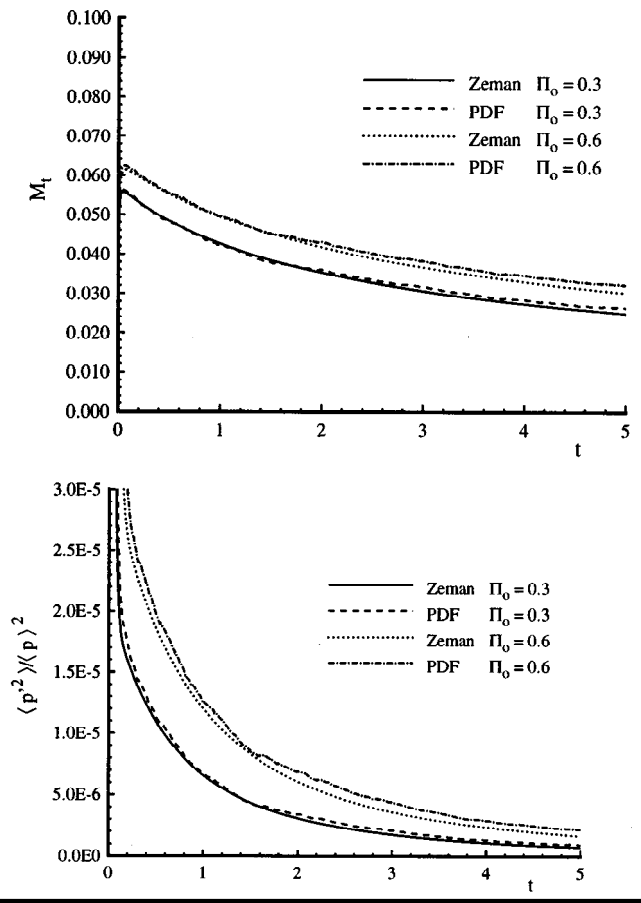


FIG. 2. Turbulent Mach number and normalized pressure variance versus time for the initial turbulent Mach number $M_{t0}=0.05$ and various values of the initial level of pressure fluctuations Π_0 .

data by Sarkar *et al.*¹³ Though this reference contains seven different run conditions, there is only one set of initial conditions consistent with our modelling assumptions.

Figure 4 shows a reasonable agreement with the data. These results are to be considered with much care, considering the limitations mentioned in section II. In particular, the reduction in the shear stress anisotropy which leads to a re-

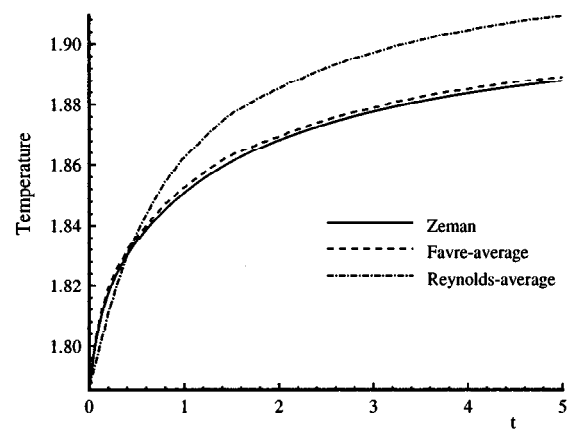


FIG. 3. Reynolds versus Favre averaged temperatures, in the case $M_{t0}=0.5$, $\Pi_0=0.05$.

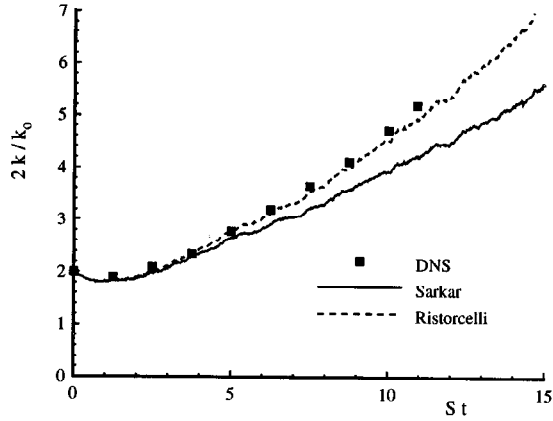


FIG. 4. Turbulent kinetic energy versus normalized time. $M_{to}=0.3$, $\Pi_0=0.005$. Solid line, PDF results based on Sarkar's model for ε_d . Dashed line, PDF results based on Ristorcelli's model for ε_d .

duced production¹⁹ is not accounted for. The good agreement of fig. 4 is therefore attributable in part to an excessive dissipation. However, since we aim to reproduce basic effects of compressibility such as the decreased growth rate of a compressible mixing layer, it is important that our model yields the correct evolution for the turbulent kinetic energy.

We also implemented a model by Ristorcelli¹⁷ for the compressible dissipation ε_d , which yields a better agreement. We nevertheless decided to retain the Sarkar *et al.* model¹¹ in the following sections.

V. INHOMOGENEOUS FLOWS: THE COMPRESSIBLE PLANE MIXING LAYER

A. The mean pressure problem

A basic problem in PDF/Monte Carlo methods over the past decade has been the determination of the mean pressure field. One issue is the reduction of statistical noise, inherent to Monte Carlo simulations. Another one is the enforcement, at the stochastic particle level, of mass conservation. Both problems have been addressed³⁶ through the use of a pressure algorithm based on the steady-state mean continuity equation to determine the mean pressure field.

In our case, the particle average of p^* , which evolves according to eq. (5), yields a pressure field which is extremely close to the true pressure field $\langle p \rangle$, and addresses the issue of mass conservation at the particle level — the analysis is rather lengthy and outside the scope of this paper. However, this particle averaged field contains considerable statistical noise, and we have to modify our approach in inhomogeneous flows to eliminate this problem. The following analysis is valid in steady flows only.

In the modified formulation, each particle is no longer assigned a full pressure p^* , but a *fluctuating pressure* p'^* such that

$$\langle p' \rangle = 0.$$

The total pressure is recovered using

$$p^* = \langle p \rangle + p'^*,$$

where $\langle p \rangle$ is the mean pressure field, defined at grid points throughout the domain, and obtained using a separate algorithm. Hence our PDF formulation is implemented in the framework of a so-called particle-mesh method. At this point it is important to note that the method described below to obtain the pressure is not a full Navier–Stokes solver. It is based on the solution of an elliptic equation for the pressure on a given grid, using information supplied by the set of stochastic particles. Other statistics, for example, the mean velocity, are not solved for in the same way, but are averaged over the individual stochastic particle properties.

The evolution equation for p'^* is derived from eq. (18):

$$dp'^* = dp^* - U^* \cdot \nabla \langle p \rangle dt, \quad (27)$$

where dp^* is given by eq. (18). The average of the pressure fluctuations evolving according to (27) is zero in steady flows. The evolution equation for $\langle p'^2 \rangle$ is not modified. The sole difference between this approach and the approach detailed in the previous sections is that the mean pressure $\langle p \rangle$ is obtained by a pressure algorithm which makes it possible to filter out the statistical error. The resulting pressure field does, however, obey the steady-state version of eq. (5).

To obtain the mean pressure, we base our approach on the steady-state mean continuity equation:

$$\nabla \cdot \langle \rho U \rangle = 0. \quad (28)$$

The idea of the algorithm is to correct the mean pressure $\langle p \rangle$ at each time step dt and at each grid point by an amount $\delta \langle p \rangle$ so that (28) is satisfied at all times. The pressure correction brings about a density correction $\delta \rho$ (which we specify to take place at a constant specific energy), and a velocity correction δU . These corrections are given by the following formulae:

$$\delta \rho = \frac{1}{(\gamma - 1) \bar{e}} \delta \langle p \rangle, \quad (29)$$

$$\delta U = - \frac{1}{\langle \rho \rangle} \nabla (\delta \langle p \rangle) dt. \quad (30)$$

Substituting for $\rho + \delta \rho$ and $U + \delta U$ in (28), we obtain the equation for $\delta \langle p \rangle$:

$$\nabla \cdot \left(\gamma \frac{U}{a^2} \delta \langle p \rangle \right) - \nabla^2 (\delta \langle p \rangle) dt = - \nabla \cdot \langle \rho U \rangle. \quad (31)$$

This equation is solved at each time step for $\delta \langle p \rangle$. The particular form of the 9-point Laplacian operator in this particle-mesh discretization makes it necessary to filter the solution to remove an instability whose wavelength is twice the grid size. This is done by using a simple centered filter, where the value of the solution at a grid point is replaced by the weighted average of the values at the point and its north, south, east, and west neighbors. The solution is finally smoothed to reduce statistical error, by using a standard fourth-order artificial viscosity method. The mean pressure $\langle p \rangle$ is then updated. In the process, mass conservation is enforced at the particle level. The particular way in which

the density is corrected (at constant temperature) is arbitrary but does not have any influence on the steady-state pressure or density fields.

The first term in the left-hand side of eq. (31) accounts for all compressibility effects on the mean pressure field, including shocks and steady acoustic waves. The second term is analogous to the Laplacian operator in the Poisson equation for pressure in incompressible flows. It can be shown that the first term is of order M^2 compared to the second, where M is a characteristic Mach number. Therefore in the limit of small M , we recover the Poisson equation for pressure. In this approach, the pressure is considered as the agent through which mass conservation is enforced.

With this new approach, the pressure–dilatation correlation is still the average of the fluctuating pressure work, and the pressure variance evolution equation is unmodified. Furthermore, the mean pressure field $\langle p \rangle$, although smoother, still satisfies the steady-state version of eq. (5). Therefore the only limitation that we have introduced is the restriction of the method to steady compressible flows.

B. Growth rate calculations

The dimensional parameters needed to describe a mixing layer between two streams made of ideal gases are the free-stream velocities U_i , pressures p_i , densities ρ_i , specific heat ratios γ_i , and specific gas constants R_i , where $i=1,2$ correspond to the high- and low-speed streams, respectively. The corresponding nondimensional parameters are

$$\frac{\gamma_2}{\gamma_1}, \frac{p_2}{p_1}, \frac{\rho_2}{\rho_1}, \frac{R_2}{R_1}, \gamma_1, \frac{U_2}{U_1}, M_1.$$

For our growth rate calculations, we set the first four parameters to 1, and take $\gamma_1=1.4$. Under these conditions it is convenient, in place of M_1 , to use the *convective Mach number* M_c defined as^{3,37}

$$M_c = \frac{U_1 - U_2}{2a}, \quad (32)$$

where a is the speed of sound, identical in both streams. The spreading rate of the shear layer in the self-similar region is a nondimensional constant, and therefore it is related to the only varying nondimensional parameters by

$$\delta' = \frac{d\delta}{dx} = f\left(\frac{U_2}{U_1}, M_c\right). \quad (33)$$

The mixing layer width δ is defined as the 0.1–0.9 thickness, which is the distance between the points at which the mean velocity is $U_2 + 0.1\Delta U$ and $U_2 + 0.9\Delta U$, respectively. To measure the effects of compressibility on δ' , we measure the quantity δ'/δ'_0 where δ'_0 is the incompressible growth rate at the same velocity ratio, obtained by setting M_c to zero in (33). Replacing M_1 by M_c in the initial set of nondimensional parameters has the effect that δ'/δ'_0 is a very weak function of the velocity ratio.³

It is emphasized at this point that the above dimensional analysis contains no large-scale structures considerations. It has been found⁶ that the convective Mach number, whose existence depends on such structures,^{3,37} is not always de-

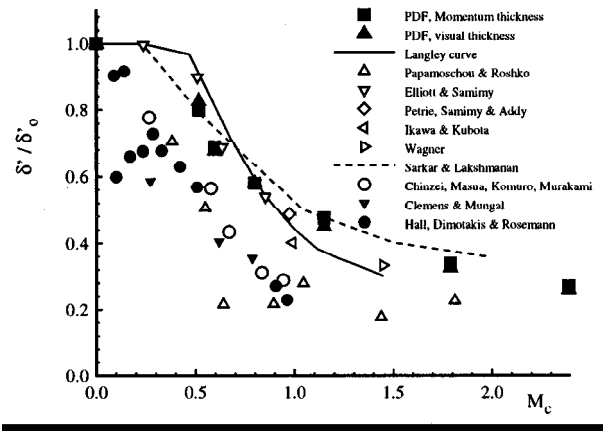


FIG. 5. Growth rate reduction with increasing M_c . The big symbols are for the present calculations, for both the momentum and the 0.1–0.9 thicknesses. The figure was partly reproduced from Ref. 33.

finer, and much less unique, in highly compressible flows. In our case, however, the parameter M_c defined by (32) can always be substituted for M_1 if the thermodynamic properties are matched in both streams, to the effect that the growth rate ratio δ'/δ'_0 is a weaker function of U_2/U_1 . M_c will therefore correlate very well the effects of compressibility on the shear layer growth rate, independently of the velocity ratio.

Figure 5 shows the present calculated growth rates compared to experimental data and computer simulations. The velocity ratios varied, for these calculations, between 0.2 and 0.5. Our results are close to those of Sarkar and Lakshmanan,²⁹ as can be expected since the compressibility effects — namely, the compressible dissipation — are modelled in the same way. In an attempt to bring the calculated growth rates closer to the general scatter than Sarkar and Lakshmanan did, the value of C_d that we chose was 2, and theirs was 1, which accounts for the slight discrepancy between the two curves. Overall, our results still lie in the upper region of the scatter.

Figures 6 and 7 show the effect of convective Mach number on the self-similar turbulence profiles, here $\langle u'^2 \rangle$ and $\langle u'v' \rangle$. The velocity ratio was set to 0.5 for all the runs,

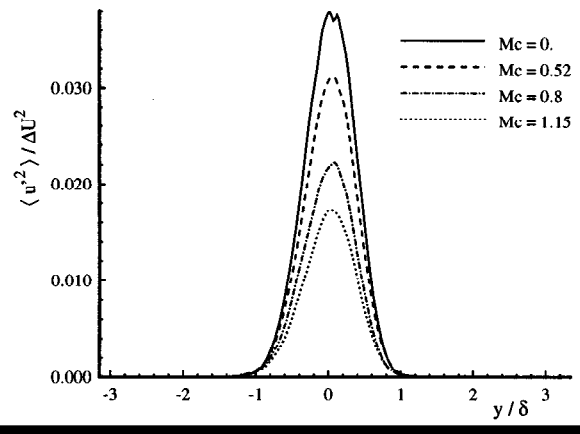


FIG. 6. The effect of M_c on self-similar streamwise turbulence intensity.

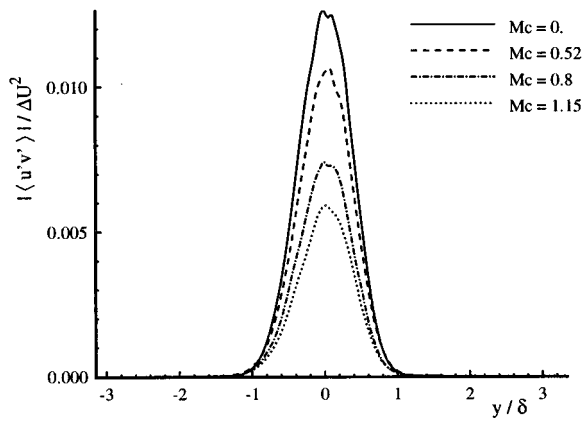


FIG. 7. The effect of M_c on self-similar Reynolds shear stress.

therefore only M_c varies. Compressibility reduces the intensity of the turbulence in a symmetric way, over the whole width of the layer. Shown for comparison are the incompressible profiles ($M_c = 0$) for the same velocity ratio. We can see that the growth rate reduction is attributable, with our model, to an overall decrease in the turbulence intensity across the layer.

C. Comparison with experimental data

In this section we compare our results with experimental data by Samimy *et al.*^{4,5,7} and Dutton *et al.*^{8,9} Although growth rate measurements are abundant in the literature, it is not so for mean and turbulent velocity profiles. The above references were the only ones known to the authors at the time of writing.

In both sets of experiments, the convective Mach number was varied simultaneously with the pressure ratio, density ratio, and velocity ratio. Though Dutton *et al.* studied seven cases in all, and Samimy *et al.* three, we chose two cases out of each set with similar convective Mach numbers: 0.46 and 0.86 in the Dutton *et al.* experiments (cases 2 and 4^{8,9}) and 0.51 and 0.86 in the Samimy *et al.* experiments (cases 1 and 3^{4,7}). For each case we ran the PDF code with the corresponding set of nondimensional parameters. Our results will therefore allow us not only to assess the performance of the PDF model, but also to compare both sets of experimental results. The nondimensional parameters corresponding to each case are summarized in table I.

Figure 8 shows the mean streamwise velocity profiles, in

TABLE I. Nondimensional parameters for Samimy *et al.* and Dutton *et al.* experiments.

Case	Samimy 1	Dutton 2	Samimy 3	Dutton 4
U_2/U_1	0.36	0.57	0.25	0.16
p_2/p_1	1.03	1	1	1
ρ_2/ρ_1	0.64	1.55	0.37	0.60
R_2/R_1	1	1	1	1
γ_2/γ_1	1	1	1	1
γ_1	1.4	1.4	1.4	1.4
M_1, M_2	1.80, 0.51	1.91, 1.36	3.01, 0.45	2.35, 0.30
M_c	0.51	0.46	0.86	0.86

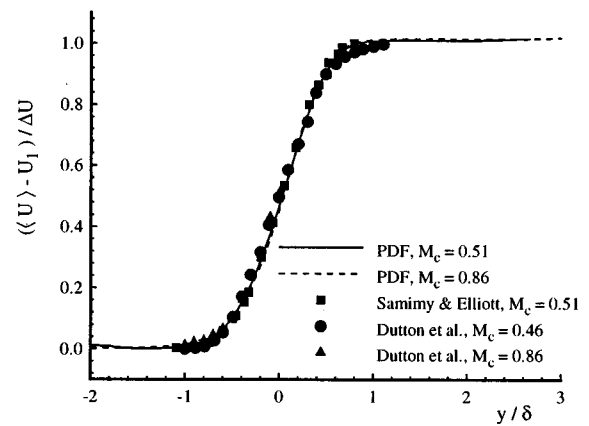


FIG. 8. Mean streamwise velocity profiles in the self-similar region.

the self-similar region, for a subset of cases: case 1 for Samimy *et al.*, cases 2 and 4 for Dutton *et al.*, and the PDF runs corresponding to the Samimy cases. The other cases are not shown for the sake of not overloading the plot. As is evident on the figure, the profiles collapse very well on a single curve. It was observed, in both the PDF calculations and the experiments, that the mean streamwise velocity profiles became self-similar earlier than the turbulent stress profiles.

Figures 9 and 10 show the streamwise turbulence intensity for the PDF calculations and the experiments. It is found that the agreement is excellent with the Samimy *et al.* results, but not as good for the Dutton *et al.* results. In fact, Dutton *et al.* found that the streamwise turbulent intensity showed very little variation with M_c , which was not the case for Samimy *et al.* Our results are closer to the findings of Samimy *et al.*, though the model does not seem to reproduce the preferential decrease in turbulence intensity in the high-speed side.

Figures 11 and 12 show the Reynolds shear stress for the PDF calculations and the experiments. Again, the agreement is very good with the Samimy *et al.* data, and not as good for the Dutton *et al.* set, though better than in the previous plot.

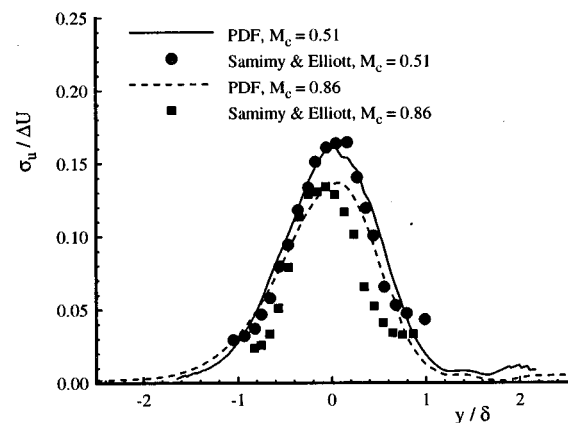


FIG. 9. Streamwise turbulent intensity. A comparison between PDF calculations and Samimy *et al.* data.

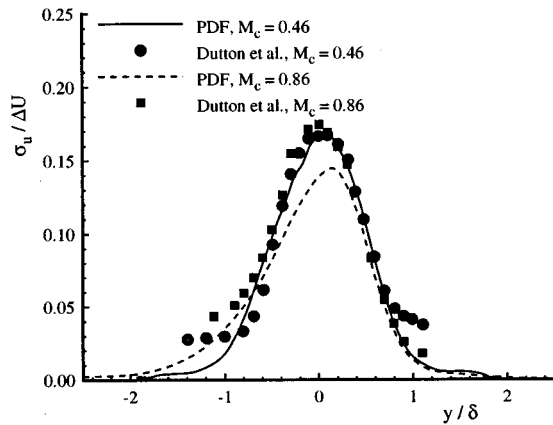


FIG. 10. Streamwise turbulent intensity. A comparison between the PDF calculations and Dutton *et al.* data.

This is to be expected, since it has been shown³⁸ that in compressible mixing layers the normalized Reynolds shear stress scales with the normalized growth rate. The closer agreement, in this case, between our calculations and the Dutton *et al.* data is therefore a consequence of the agreement between our growth rate calculations and the general scatter, as shown in fig. 5.

Figure 13 shows the lateral convection of turbulent kinetic energy. It is a third moment, and therefore easily calculated if one knows the one-point density-weighted joint PDF \tilde{f} . The agreement between our calculations and experimental results is reasonable, but not as good as for the second moments: the PDF model seems to underpredict the importance of this transport term. This might contribute to the observed smaller value of the turbulence intensity in the edges of the layer in the PDF calculations, as is evident in figs. 9 and 10. We should, however, mention the importance of statistical noise in both our calculations and the experiments, which becomes larger as one measures higher-order moments. The sampling region over which the third moment was calculated contained approximately 10000 particles, which is the maximum that could be reached while achieving

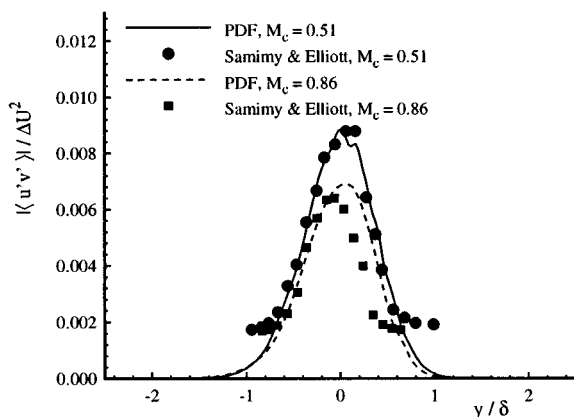


FIG. 11. Reynolds shear stress. A comparison between the PDF calculation and Samimy *et al.* data.

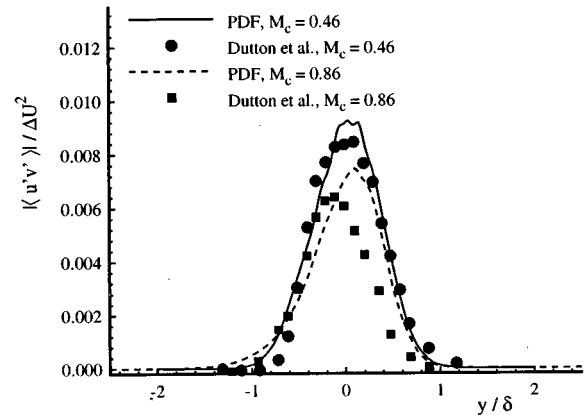


FIG. 12. Reynolds shear stress. A comparison between the PDF calculation and Dutton *et al.* data.

reasonable run times. Samimy and Elliott used 4096 samples. A minimum number of samples for this moment would be around four times as much.⁴ Therefore in both the calculations and the experiments the minimum number of samples was not reached, and statistical error is still important.

Figure 14 shows the correlation coefficient between the streamwise and the lateral turbulent velocity fluctuations. Both experiments show that the correlation coefficient is weakly affected by compressibility. We compared in this case the results with different PDF calculations, done at $M_c = 0$ and $M_c = 1.15$. It is found that not only does the correlation coefficient vary weakly with M_c , it is also very close to the incompressible value across the whole layer. Future turbulence models for compressibility effects should therefore attempt to reproduce this result, which is common to both sets of experiments.

Overall, it is found that the agreement with experimental data is very good for the Samimy *et al.* set, and reasonable for the Dutton *et al.* set. The limited amount of available data, however, precludes us from drawing extensive conclusions.

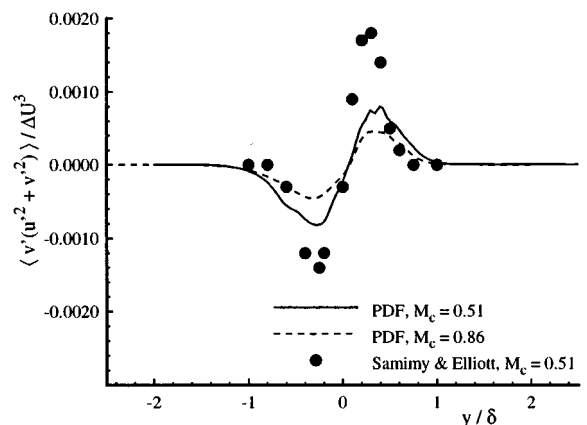


FIG. 13. Lateral convection of turbulent kinetic energy in the self-similar region.

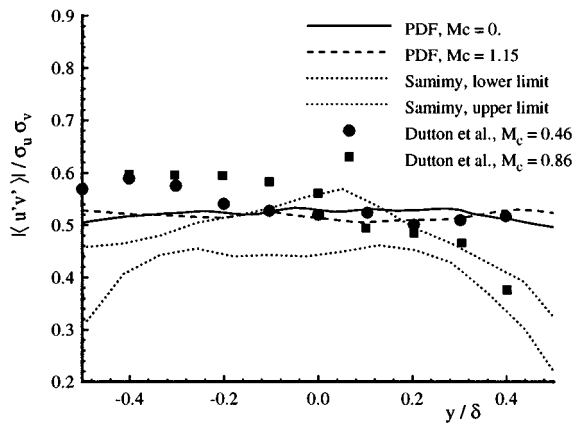


FIG. 14. The correlation coefficient for u' and v' in the self-similar region. For the Samimy results, we show the lower and upper limit of the scatter.

VI. CONCLUSIONS

We have presented a new model that extends the applicability of methods based on the joint probability density function to compressible flows. The method is based on a modelled transport equation for the joint PDF of velocity, turbulent frequency, pressure (or fluctuating pressure), and specific internal energy. We have tested this model in both homogeneous and inhomogeneous flows, in the Monte Carlo simulation framework, and have found good agreement between our results and available data in both cases. In the inhomogeneous case, we have designed and implemented an algorithm to obtain the mean pressure while filtering out the statistical noise and enforcing mass conservation at the stochastic particle level. This algorithm is applicable to flows with arbitrary pressure gradients as well as to recirculating flows. The compressibility aspects of the turbulence modelling are based, largely, on existing Reynolds stress closures.^{11,15} Consequently, the PDF model inherits several performance characteristics of these Reynolds stress models. As improved Reynolds stress models are developed — to account for the effects of compressibility on the pressure-rate of strain correlation, for example — it will be straightforward to incorporate these improvements in the PDF model.

The present model is valid for inert flows. Our long-term goal, however, is to predict the properties of supersonic reacting flows, in the context of high-speed combustion. The extension of our present approach to reacting flows is expected to be straightforward, and will be the next step to be taken by the authors.

ACKNOWLEDGMENT

This work was supported by Grant No. NAG 1 1542 from the NASA Langley Research Center, Program Manager Dr. Phil Drummond.

¹S. K. Lele, “Compressibility effects on turbulence,” *Annu. Rev. Fluid Mech.* **26**, 211 (1994).

²N. T. Clemens and M. G. Mungal, “Large-scale structure and entrainment in the supersonic mixing layer,” *J. Fluid Mech.* **284**, 171 (1995).

³D. Papamoschou and A. Roshko, “The compressible turbulent shear layer: An experimental study,” *J. Fluid Mech.* **197**, 453 (1988).

- ⁴M. Samimy and G. S. Elliott, “Effects of compressibility on the characteristics of free shear layers,” *AIAA J.* **28**, 439 (1990).
- ⁵M. Samimy, M. F. Reeder, and G. S. Elliott, “Compressibility effects on large structures in free shear flows,” *Phys. Fluids A* **4**, 1251 (1992).
- ⁶D. Papamoschou, “Structure of the compressible turbulent shear layer,” *AIAA J.* **29**, 680 (1990).
- ⁷G. S. Elliott and S. Samimy, “Compressibility effects in free shear layers,” *Phys. Fluids A* **2**, 1231 (1990).
- ⁸S. G. Goebel and J. C. Dutton, “Experimental study of compressible turbulent mixing layers,” *AIAA J.* **29**, 538 (1990).
- ⁹S. G. Goebel, J. C. Dutton, H. Krier, and J. P. Renie, “Mean and turbulent velocity measurements of supersonic mixing layers,” *Exp. Fluids* **8**, 263 (1990).
- ¹⁰R. Abid, “On prediction of equilibrium states in homogeneous compressible turbulence,” Technical report, NASA Contractor Report 4570, 1994.
- ¹¹S. Sarkar, G. Erlebacher, M. Y. Hussaini, and H. O. Kreiss, “The analysis and modelling of dilatational terms in compressible turbulence,” *J. Fluid Mech.* **227**, 473 (1991).
- ¹²S. Sarkar, “The pressure-dilatation correlation in compressible flows,” *Phys. Fluids B* **4**, 2674 (1992).
- ¹³S. Sarkar, G. Erlebacher, and M. Y. Hussaini, “Direct simulation of compressible turbulence in a shear flow,” *Theor. Comput. Fluid Dyn.* **2**, 291 (1991).
- ¹⁴O. Zeman, “Dilatation dissipation: The concept and application in modeling compressible mixing layers,” *Phys. Fluids A* **2**, 178 (1990).
- ¹⁵O. Zeman, “On the decay of compressible isotropic turbulence,” *Phys. Fluids A* **3**, 951 (1991).
- ¹⁶O. Zeman and G. Coleman, “Compressible turbulence subjected to shear and rapid compression,” in *Turbulent Shear Flows 8* (Springer-Verlag, Berlin, 1993), p. 283.
- ¹⁷J. R. Ristorcelli, “A pseudo-sound constitutive relationship and closure for the dilatational covariances in compressible turbulence: An analytical theory,” submitted to *J. Fluid Mech.*
- ¹⁸C. Cambon, G. N. Coleman, and N. N. Mansour, “Rapid distortion analysis and direct simulation of compressible homogeneous turbulence at finite Mach number,” *J. Fluid Mech.* **257**, 641 (1993).
- ¹⁹S. Sarkar, “The stabilizing effect of compressibility in turbulent shear flow,” *J. Fluid Mech.* **282**, 163 (1995).
- ²⁰S. B. Pope, “Pdf methods for turbulent reactive flows,” *Prog. Energy Combust. Sci.* **11**, 119 (1985).
- ²¹S. M. Correa and S. B. Pope, “Comparison of a Monte Carlo pdf/finite-volume mean flow model with bluff-body Raman data,” in *24th International Symposium on Combustion* (The Combustion Institute, Pittsburgh, 1992), p. 279.
- ²²G. C. Chang, “A Monte Carlo PDF/All-speed finite-volume study of turbulent flames,” Ph.D. thesis, Cornell University, 1995.
- ²³S. B. Pope and Y. L. Chen, “The velocity-dissipation probability density function model for turbulent flows,” *Phys. Fluids A* **2**, 1437 (1990).
- ²⁴S. B. Pope, “Application of the velocity-dissipation probability density function model to inhomogeneous turbulent flows,” *Phys. Fluids A* **3**, 1947 (1991).
- ²⁵A. T. Hsu, Y.-L. P. Tsai, and M. S. Raju, “Probability density function approach for compressible turbulent reacting flows,” *AIAA J.* **7**, 1407 (1994).
- ²⁶C. Dopazo, “Recent developments in pdf methods,” in *Turbulent Reacting Flows*, edited by P. A. Libby (Academic, New York, 1994), Chap. 7.
- ²⁷W. C. Welton and S. B. Pope, “A pdf-based particle method for compressible turbulent flows,” *AIAA Paper No. 95-0804*, 1995.
- ²⁸G. Erlebacher, M. Y. Hussaini, H. O. Kreiss, and S. Sarkar, “The analysis and simulation of compressible turbulence,” *Theor. Comput. Fluid Dyn.* **2**, 73 (1990).
- ²⁹S. Sarkar and B. Lakshmanan, “Application of a Reynolds stress turbulence model to the compressible shear layer,” *AIAA J.* **29**, 743 (1991).
- ³⁰A. W. Vreman, N. D. Sandham, and K. H. Luo, “Compressible mixing layer growth rate and turbulence characteristics,” *J. Fluid Mech.* **320**, 235 (1996).
- ³¹Jayesh and S. B. Pope, “Stochastic model for turbulent frequency,” Technical report, FDA 95-05, Cornell University, 1995.
- ³²W. Kollmann, “The pdf approach to turbulent flow,” *Theor. Comput. Fluid Dyn.* **1**, 249 (1990).

- ³³K. N. C. Bray, P. A. Libby, and F. A. Williams, "High speed turbulent combustion," in *Turbulent Reacting Flows*, edited by P. A. Libby (Academic, New York, 1994), Chap 10.
- ³⁴D. C. Haworth and S. B. Pope, "A generalized Langevin model for turbulent flows," *Phys. Fluids* **29**, 387 (1986).
- ³⁵S. B. Pope, "On the relationship between stochastic Lagrangian models of turbulence and second-moment closures," *Phys. Fluids* **6**, 973 (1994).
- ³⁶S. B. Pope, "Position, velocity and pressure correction algorithm for particle method solution of the pdf transport equations," Technical report, FDA 95-06, Cornell University, 1995.
- ³⁷D. W. Bogdanoff, "Compressibility effects in turbulent shear layers," *AIAA J.* **21**, 926 (1983).
- ³⁸G. L. Brown and A. Roshko, "On density effects and large structures in turbulent mixing layers," *J. Fluid Mech.* **64**, 775 (1974).